Solvation at Surfaces and Interfaces: a Quantum-Mechanical/Continuum Approach Including Non-Electrostatic Contributions

Krzysztof Mozgawa,[†] Benedetta Mennucci,[‡,¶] and Luca Frediani[*,†]

Centre of Theoretical and Computational Chemistry, Department of Chemistry, University of Tromsø,N-9037 Tromsø, Norway, and Dipartimento di Chimica e Chimica Industriale, University of Pisa, 56126 Pisa , Italy

E-mail: luca.frediani@uit.no

[*]To whom correspondence should be addressed

[†]Centre of Theoretical and Computational Chemistry, Department of Chemistry, University of Tromsø,N-9037 Tromsø, Norway

[‡]Dipartimento di Chimica e Chimica Industriale, University of Pisa, 56126 Pisa , Italy

[¶]Centre of Theoretical and Computational Chemistry, Department of Chemistry, University of Tromsø,N-9037 Tromsø, Norway

Abstract

We present an integrated QM/classical approach to treat solvation at diffuse solvent surfaces and interfaces within the framework of continuum solvation models. Solvation energy is divided into electrostatics, dispersion, repulsion and cavitation contributions which are all modeled within a QM formulation with the exception of cavitation. The model is tested by studying solvation energy profiles of small molecules and comparing them with atomistic simulations available in the literature. The good agreement found in the two investigated sets of systems indicate both the feasibility and the semiquantitative accuracy of the approach.

Keywords

Green's function, Dispersion, Repulsion, Cavitation, Boundary equation, Surfactant

1 Introduction

The foundation of continuum solvation models is the subdivision of the total system into a molecular solute (generally a single molecule unless specific interactions such as hydrogen bonding or π-stacking demand a supermolecular approach) and a continuum solvent which is assumed to be infinite and structureless. Within this framework, transfer of the solute from the gas phase to a liquid is traditionally broken into two steps, first the formation of a cavity in the bulk of the liquid and then the insertion of the solute in the cavity. The balance between the reversible work of these two steps gives, according to this model, the excess free energy of the process or, in other words, the solvation free energy G^{sol}. Adopting such a strategy, G^{sol} can be obtained by resorting to a partition into four separate, but in principle coupled, terms, namely:

$$G^{sol} = G^{el} + G^{rep} + G^{dis} + G^{cav} \tag{1}$$

where G^{el}, G^{rep}, G^{dis} represent the contribution of electrostatic, repulsion and dispersion interactions, respectively and G^{cav} refers to the the energy involved in the first step, namely the cavitation energy.

During the years, many different formulations have been proposed to compute G^{cav}. Nowadays, two alternative families of approaches are in use: those based on statistical mechanics and those based on the area of the solute exposed to the solvent.[1,2] As regards the second step of the process, short-range interactions such as dispersion and Pauli-like repulsion and long-range electrostatic interactions come into play. Electrostatic interactions do not introduce real theoretical difficulties, as they represent the classical interactions between the charges of the solute and those of the solvent. The challenging contributions are dispersion and repulsion since they are deeply rooted in the quantum-mechanical (QM) nature of the overall system and their accurate treatment is difficult to achieve even with QM approaches commonly used to describe molecular properties and processes. Several strategies have been followed, depending on the problem investigated. For intra- and intermolecular interactions in a fully QM system, Grimme has developed a correction to the energy in connection with some commonly used density functionals.[3] For condensed systems, Gordon and coworkers[4] have included dispersion and repulsion effects in their Effective Fragment Potential (EFP) approach. The additional difficulty for continuum models is the lack of an atomistic description of the solvent which is the basis for all the approaches followed in the aforementioned methods. A possible way around can be found by comparing dispersion and repulsion to electrostatics, for which both continuum and atomistic descriptions are available. The expression for dispersion and repulsion can hence be heuristically derived. Adopting such a strategy, continuum solvation models have been widely and successfully used for estimating solvation free energies.

Nowadays continuum solvation models are largely used in combination with a quantum-mechanical (QM) description of the solute.[1,2,5] However, in most of the different QM/continuum strategies developed so far, a semiclassical approach is generally used for the non-electrostatic

terms, namely they enter in the definition of the solvation free energy but not in the QM formulation of the model. More in detail, dispersion and repulsion components have been determined using classical expressions, which mainly rely on the use of (i) pair potentials expressed as truncated expansions in powers of $1/r$ that relate suitable chemical fragments of solute and solvent molecules,[6] or alternatively (ii) empirical expressions related to the solvent-exposed surface of atoms.[7–9] Very recently a new kind of treatment of the solute-solvent dispersion contribution to the solvation free energy has been proposed: this model utilizes two descriptors, namely, the spherically averaged dipole polarizability of the solute molecule (either in its ground or excited electronic state) and the refractive index of the solvent.[10] QM-based strategies to compute repulsion and dispersion effects have been proposed within the Polarizable Continuum Model (PCM) family.[2] According to this formulation, the repulsion and dispersion effects can be explicitly included in the effective Hamiltonian together with the electrostatic one, and as a result the solute wavefunction (i.e. the electronic density) will be explicitly affected by both electrostatic and non-electrostatic effects. This formulation, originally due to Amovilli and Mennucci,[11] can be considered a generalization of the theory of intermolecular forces to the specific case of a solute embedded in a cavity surrounded by a continuum solvent. The original formulation was optimized for the Hartree-Fock formulation but more recently, the same method has been reformulated for a Density Functional Theory (DFT) description of the solute and extended to treat electronic transitions.[12] A similar approach has recently been proposed by Pomogaeva and Chipman,[13] who formulated the dispersion interaction in terms of the electron density of the solute, mutuating a recent development in Density Functional Theory (DFT) to include dispersion effects which are generally missing in most functionals.[3,14]

In this paper we make a further step towards a more general applicability of continuum solvation models to molecular problems of increasing complexity and we focus on a full QM formulation of the PCM approach for non-homogeneous environments such as gas-liquid and liquid-liquid interfaces. In previous papers we have shown that the electrostatic component

of the PCM approach when formulated within the integral equation formalism (IEF)[15,16] can be applied to very different media ranging from standard isotropic solvents characterized by a scalar permittivity to anisotropic dielectrics such as liquid crystals and polymers, passing through liquid-liquid, liquid-gas, or liquid-solid interfaces or planar membranes.[17] However, as far as it concerns non-electrostatic terms, there is not a complete and coherent treatment going beyond the isotropic media. A few years ago, two of the present authors extended the Amovilli and Mennucci approach for repulsion interactions to interfaces;[18] now this extension is completed by adding the dispersion and cavitation terms. Within this new formulation electrostatics, repulsion and dispersion are all coupled together with the QM description of the solute charge density and their effects are properly included not only in the determination of the solvation free energy but also in the calculation of molecular response properties. The contribution of cavitation is instead kept separated from the QM determination of the solute wavefunction and evaluated at classical level using only the geometrical characteristics of the solute system.

The paper is organized as follows: first we report the methodological approach developed to generalize dispersion and cavitation to non-homogeneous dielectrics and successively we present some applications of the same method to several series of calculations for the free energy of phase transfer for liquid-liquid and liquid-vacuum interfaces.

2 Methods

In the Introduction we have reported the commonly accepted picture which divides the solute-solvent interactions into electrostatics, dispersion, repulsion, and cavitation terms as shown in Eq. 1. A further step is however necessary in order to generalize such an approach to surfaces and interfaces since two different solvents have now to be accounted for. As electrostatics and repulsion interactions have been already presented and discussed in previous papers;[17–19] in this section we will mostly focus on cavitation and dispersion terms. For both of them,

first we shall briefly summarize how they are computed for a homogeneous, isotropic solvent, and then we shall present a more detailed extension to surfaces and interfaces.

2.1 Electrostatics and repulsion

Electrostatics is the most commonly employed term in the context of solute-solvent interactions. The inclusion of such effect into quantum chemistry programs started in the 1970s,[20,21] whereas the first PCM formulation was presented in 1981.[22] An important generalization of the PCM was achieved with its IEF reformulation, originally developed in 1997,[15,16] which allowed for a general solution of the electrostatic problem for different environments, including sharp planar[19] and diffuse interfaces[17] between two media with different dielectric permittivities.

In short the PCM description of the electrostatic solute-solvent interaction including polarization effects is through an apparent surface charge (ASC) density $\sigma(r)$ supported on the cavity surface Γ. Within the IEF version of the model, the ASC is obtained as the solution of the following integral equation:

$$\left[\left(\frac{1}{2} - D_e\right) S_i + S_e \left(\frac{1}{2} - D_i^*\right)\right] \sigma = \left[\left(\frac{1}{2} - D_e\right) - S_e S_i \left(\frac{1}{2} - D_i\right)\right] V_i \qquad (2)$$

where V_i is the electrostatic potential generated by the molecular charge density. S_i and S_e are the so-called single-layer operators: their kernel is the electrostatic Green's function in the interior (i-subscript) and in the exterior (e-subscript) of the cavity Γ. D_i and D_e (D_i^* is the adjoint of D_i) are the double-layer operators: their kernel is the derivative of the single-layer kernel. For details about how to obtain Eq. (2) see Ref.23. We limit ourselves here to two considerations: the Green's functions of the interior is $G_i(r, r') = 1/|r - r'|$ as vacuum is assumed, whereas the Green's function of the exterior depends on the given medium; the dielectric properties of the two media (interior and exterior) together with the cavity boundary Γ fully defines the operators appearing in Eq. (2) and their successive

discretization for practical applications.

For a diffuse interface, defined as a medium with a position-dependent permittivity, the Green's function can be viewed as a sum of a Coulomb-like term and an image potential term:

$$G(r, r') = \frac{1}{c(r, r')|r - r'|} + G_{img}(r'r'). \tag{3}$$

Both the effective permittivity $c(r, r')$ and the image contribution depend on the shape of the permittivity across the interface which can be expressed as $\epsilon(z)$ being z the distance with respect to the interface. For further details we refer to the original paper.[17]

Moving to repulsion interactions, the Amovilli and Mennucci's approach[11] is here adopted. In short, within such a framework the repulsion contribution is derived from the exchange and penetration terms of the decomposition of the intermolecular interaction energy. A simplified expression for a uniform solvent, which takes into account its continuum nature is then obtained:

$$G_{rep} = \alpha \int_{\boldsymbol{r} \notin C} \mathrm{d}\boldsymbol{r} P(\boldsymbol{r}) \, \mathrm{d}r \tag{4}$$

This expression shows that the repulsion interaction is proportional to the so called "escaped charge": the electronic density which extends beyond the boundaries of the molecular cavity. For an interface, the lack of uniformity of the medium (solvent properties are now position-dependent) implies that the proportionality coefficient α is position-dependent and should be kept inside the integration. An approach to deal with such a problem has first been proposed by Frediani *et al.*[18] for spherical cavities and later refined by Bondesson *et al.*[24] for the general case. The final expression can be written as follows:

$$G_{rep} = \alpha' \int_{\Gamma} \rho(s) f(s, \gamma) n(s) \, \mathrm{d}s \tag{5}$$

where $\rho(s)$ is the electron density of the solute at the cavity surface, $f(s, \gamma)$ is a weight factor and the parameter α' collects all constant factors of the expression for a single solvent except the density of valence electrons $n(s)$ which is no longer a constant for the interfacial case.

The functional form of $f(s,\gamma)$ is described in Ref. [24], and the parameter γ is obtained through the following relation:

$$n_{out} = \int_{\Gamma} \rho(s) f(s,\gamma)\, \mathrm{d}s \tag{6}$$

where n_{out} is the total outlying charge.

2.2 Dispersion

Following Amovilli,[25] the expression for the dispersion energy in an homogeneous solvent is achieved by similarity with electrostatics. We report here the final expression for the dispersion free energy:

$$G^{disp} = \frac{1}{\pi} \int \mathrm{d}\omega \sum_{p} \frac{\omega_p}{{\omega_p}^2 + \omega^2} \int \mathrm{d}r_1 \int_{\Gamma} \frac{\mathrm{d}r_2}{|r_1 - r_2|} \rho_p(r_1) \sigma_S[\epsilon(i\omega), \rho_p](r_2) \tag{7}$$

where the index p runs over the excited states of the solute, ω_p and ρ_p are the corresponding excitation energy and transition density respectively. $\sigma_S[\epsilon(i\omega), \rho_p]$ is the ASC density induced on the cavity surface Γ by the transition charge density ρ_p depending on a dielectric constant calculated at imaginary frequencies, $\epsilon(i\omega)$. Eq. 7 has been further elaborated by Amovilli and Mennucci[11] by assuming the transition polarization charge density $\sigma_S[\epsilon(i\omega), \rho_p]$ to be proportional to the corresponding electrostatic field generated by ρ_p, namely:

$$G^{disp} = -\frac{1}{8\pi} \frac{\eta_S^2 - 1}{\eta_S^2} \sum_{p} \frac{\Omega^S}{\Omega^S + \omega_p} \int_{\Gamma} \mathrm{d}s V_p(s) E_p(s) \tag{8}$$

where V_p and E_p are the electrostatic potential and the electrostatic field associated with the transition charge density ρ_p, respectively. η_S is the solvent refractive index measured in the visible spectrum far from electron transitions whereas $\Omega^S = \eta_S I$, with I being the first ionization potential of the solvent.

In order to achieve a practical expression (one which leads to a computationally feasi-

ble expression for the Fock operator, see Ref.[11] for details), a further simplification is introduced, by making use of an averaged excitation energy ω_{ave}, thereby eliminating the dependence of the prefactor on the excited states in Eq. 8. In addition, the $1/8\pi$ factor is exchanged for an empirical correction c_f factor.

$$G^{disp} = -c_f \frac{\eta_S^2 - 1}{\eta_S^2} \frac{\Omega^S}{\Omega^S + \omega_{\text{ave}}} \int_\Gamma \mathrm{d}s \sum_p V_p(s) E_p(s) = -\beta(\omega_{\text{ave}}) \int_\Gamma \mathrm{d}s \sum_p V_p(s) E_p(s) \quad (9)$$

The original parameterization of c_f [11] was performed using Hartree-Fock calculations and the averaged excitation energy ω_{ave} was obtained by considering a predefined set of occupied and virtual orbitals defined by a window of energies and averaging for such a set. This choice is, however, strictly connected to the QM method employed; for example, it is well known that DFT and HF descriptions yield very different orbital energies when occupied and virtual orbitals are compared. As a result, the final value for ω_{ave} becomes strongly dependent on the chosen QM method.[26] In order to avoid that, a new parameterization has been more recently proposed[12] where ω_{ave} is obtained by imposing the equivalence of the dispersion energies obtained with the approximated Eq. 9 and the "exact" Eq. 7, and the fitting parameter c_f is chosen to be solvent-dependent.

The extension to surfaces and interfaces is again achieved by introducing a position dependence to $\beta(\omega_{\text{ave}})$ which collects all solvent-dependent parameters. As a result, the position-dependent β has now to be kept inside the integral over the cavity surface. The only additional complication is that the identification of the average excitation energy as in Ref.[12] must now be performed iteratively, albeit the procedure is not computationally expensive. The interface-adapted dispersion energy expression reads as follows:

$$G^{disp} = -\int_\Gamma \beta(\omega_{\text{ave}}; s) V_p(s) E_p(s)\, \mathrm{d}s \quad (10)$$

To describe the position dependence of β we have adopted the same heuristic approach of other macroscopic quantities such as the permittivity $\epsilon(z)$.[17] They all follow the same

sigmoidal profile which is borrowed from the variation of the solvent density. Within this framework, $\beta(s)$ can be rewritten as $\beta(z)$ being z the distance of the surface point s with respect to the interface. Given the two bulk values β_1 and β_2 for the two solvents, we can write:

$$\beta(z) = \frac{\beta_1 + \beta_2}{2} + \frac{\beta_1 - \beta_2}{2} \tanh\left(\frac{z - z_0}{D}\right) \tag{11}$$

where z_0 is the interface position, and D is connected to the width W of the interfacial region ($W \simeq 6D$).

As for the electrostatic and repulsion interactions, also for dispersion all the integrals on the cavity surface Γ are numerically solved by introducing a surface mesh made finite surface elements, historically called *tesserae*.

2.3 Cavitation

By definition, cavitation energy depends directly on the solvent, but only indirectly on the molecule through the cavity shape. As a consequence the model employed to compute cavitation does not contribute to the solute Hamiltonian. As said in the Introduction, several approaches have been proposed to compute cavitation contributions: these have been formulated in terms of macroscopic quantities such as surface tension and compressibility of the solvent, or they have been derived from molecular simulations, or they have exploited statistical methods (see Ref. [2] for an exhaustive list of references). The first class of approaches, gives rise to the simplest methods albeit the least accurate ones. Employing simulations would on the other hand be accurate but it is computationally very demanding, defeating the main purpose of a continuum method of being fast. The approaches based on statistical methods have instead proven to be a very good compromise between accuracy and feasibility.

The statistical method employed here is called Scaled Particle Theory (SPT) and is based on the method originally proposed by Pierotti[27] for spherical cavities. In order to adapt the

method to a molecular-shaped cavity the contribution from each sphere is multiplied by a weight which reflects the portion of the surface which is exposed to the solvent. The cavitation expression for a uniform solvent yields:

$$G_{cav} = \sum_i \omega_i G_{cav}(R_i) \tag{12}$$

where the sum runs over the spheres of the cavity, ω_i are the weight factors, and $G_{cav}(R_i)$ is the contribution from the i-th sphere.

In order to adapt the model to the case of a diffuse surface the contribution from each sphere must be further weighted with respect to the position-dependent solvent density. In practice Eq. 12 can be rearranged such that the sum will go over the tesserae instead of the spheres:

$$G_{cav} = \sum_t \frac{\rho(s_t)}{\rho_0} \frac{a_t}{4\pi R_t^2} G_{cav}(R_t) \tag{13}$$

where s_t, a_t and R_t refer respectively to the collocation point, the tessera area and R_t is the radius of the corresponding sphere. In this way the contribution from each tessera is doubly weighted, both for the surface ratio with respect to the full sphere and for its position with respect to the surface. For a molecule immersed in bulk Eq. 12 is obviously recovered. For an interface between two solvents, two such contributions need to be computed, one for each solvent. Additionally, we have included in the model a surface tension component: a molecule at the surface should reduce the solvent surface by a value corresponding to its section at the surface:

$$G_{surf} = \gamma_S A(z = 0) \tag{14}$$

where γ_S is the solvent surface tension and $A(z = 0)$ is the area of the cavity section at the interface position. In order to compute $A(z = 0)$ the following integral can be employed:

$$A = \int_\Gamma (H(z) - 1/2)\hat{z}(s) \cdot \hat{n}(s)\, \mathrm{d}s \tag{15}$$

where $H(z)$ is the Heaviside step function ($H(z) = 0$ for $z < 0$, $H(z) = 1$ for $z \geq 0$). This expression can be generalized to a diffuse surface by substituting the density ratio $\rho(z)/\rho_0$ to the step function:

$$A = \int_\Gamma (\rho(z)/\rho_0 - 1/2)\hat{z}(s) \cdot \hat{n}(s)\, \mathrm{d}s \tag{16}$$

Again we notice that the expression has the correct limit since at large distances from the interface it goes to zero.

3 Computational Details

As reported in Section 2.2, the application of the dispersion expression reported in Eq. 9 requires a parameterization of the c_f factor for each homogeneous solution. This is obtained here using as reference dispersion energies obtained with the semiclassical model[6] and adopting the same strategy proposed by Weijo et al.[12] All the details of the parameterization and the results obtained are reported in the SI.

Due to the presence of the interface, the solvation free energy becomes dependent on the position and orientation of the molecule with respect to the interface: $\Delta G = \Delta G(z, \theta, \phi)$, where z, θ and ϕ represent the distance of the molecule with respect to the interface, the angle of the main axis with respect to the normal to the interface and the rotation of the molecule around the main axis (reference position and orientation are molecule-specific). Solvation free energy profiles are obtained by keeping the orientation fixed (θ, ϕ), whereas the position z is varied across the interface. The mid-point of the interface is conventionally located at $z = 0$ (see Fig. 1).

Two sets of solutes have been analyzed:

1. Set 1: $\mathrm{CH}_x\mathrm{F}_{4-x}$ ($x = 0, 1, .., 4$).

2. Set 2: ammonia, benzene, DMSO, ethanediol, ethanol, hydrogen peroxide, methanol, nitrogen, oxygen, ozone, phenol.

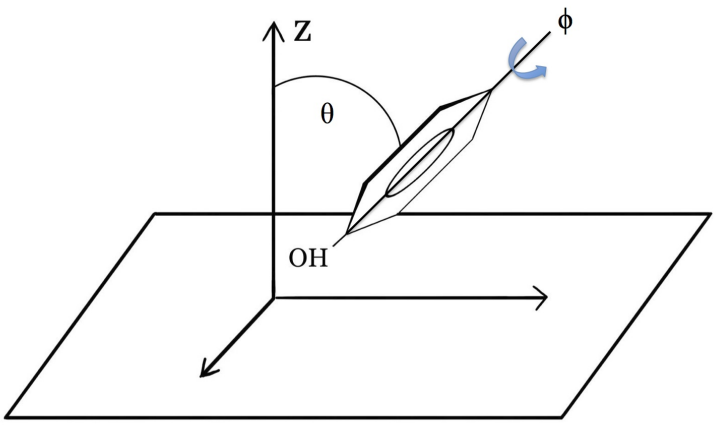

Figure 1: Graphical representation of the notation used to define the orientation of the molecular probes with respect to the surface.

For the set 1, two orientations have been explored: (i) $\theta = 0$ which refers to the orientation with the representative functional group of the given molecule pointing towards bulk water when moving from hexane to water; (ii) $\theta = 180°$ which refers to the opposite orientation. For set 2, the same orientational analysis (where applicable) was performed, with orientation $\theta = 0$ this time referring to representative functional pointing towards the liquid interface when moving from vapor to water. A more extensive orientational analysis for phenol and ethanol was also performed.

For all calculations, including geometry optimizations, we have employed the B3LYP functional[28,29] as implemented in the Gaussian03[30] program and the aug-cc-pVDZ[31] basis set. All geometries were optimized in the gas-phase and kept frozen in solution. In all calculations the free energy has been obtained without including thermal corrections (namely vibrational and rotational terms).

PCM molecular cavities have been constructed with atom-centered interlocking spheres using the following set of radii throughout: 1.6Å for nitrogen, 1.2Å for hydrogens capable of hydrogen bonding (-OH, -NH_2) 1.52Å for oxygen, 1.85Å for sulfur and 1.8Å for carbon. For -CH, -CH_2 and -CH_3 groups, a common sphere centered on carbon has been employed with radii of 1.9Å, 2.0Å and 2.1Å respectively. All radii are multiplied by the common scaling

factor of 1.2.

4 Results

We have performed two series of calculations for the free energy of phase transfer for liquid-liquid and liquid-vacuum interfaces. The first set (Set 1) has been chosen in order to compare our results to a previous study by Pohorille and Wilson[32] who simulated the phase-transfer through a water-hexane interface whereas the second set (Set 2) has been chosen to compare with the results compiled by Garrett *et al.* [33] on the free energy of water-vapor transfer. For the latter set the simulation results have been obtained by different authors: for methanol see Refs. 34 and 35, for ethanol see Ref.35, 36 and 37, for ethanediol see 37, for benzene see Ref.38, for ammonia see 39, for hydrogen peroxide, nitrogen and oxygen see 40, for ozone see 41 and 40. For the sake of simplicity, we will in the following refer to the review from Garrett *et al.* [33] when discussing data of Set 2.

For most molecules, two orientations were analyzed: $\theta = 0$ and $\theta = 180°$, taken by aligning a bond (e.g. the C−O bond for alcohols) along the z direction. For apolar molecules (CH_4, CF_4) only one orientation was considered. Additional orientations were included if specified.

4.1 Solvation energy profiles of Set 1

In Fig. 2 we report the solvation free energy profiles of the $CH_xF_{(4-x)}$ molecules belonging to Set 1 at the water-hexane interface.

The zero of energy is set to the energy of each molecular system in gas-phase. In Fig. 2 positive z values correspond to the molecule in hexane whereas negative values to the molecule in water.

The solvation profiles show that the more polar molecules (CHF_3, CH_3F and CH_2F_2) have a clear surfactant behavior with energy minima between 1 and 2 kcal/mol when the solvation free energy in bulk water is taken as a reference. On the contrary, CF_4 and methane

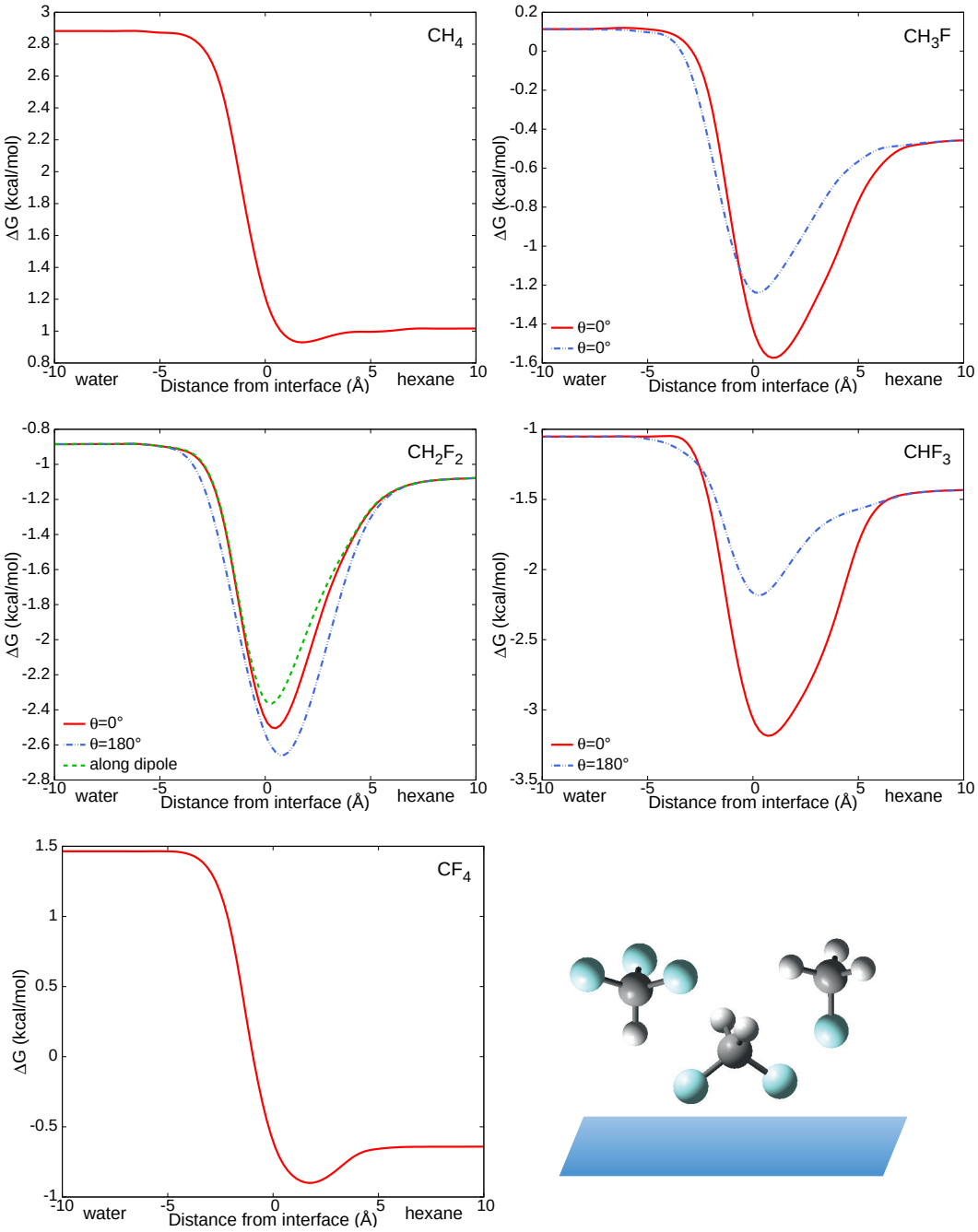

Figure 2: Solvation free energy profiles (in kcal/mol) for the $CH_xF_{(4-x)}$ set of molecules at the water-hexane interface. The full and the dotted lines refer to $\theta = 0$ and $\theta = 180°$ orientations, respectively. For CH_2F_2 a third profile is shown referring to the orientation of the solute with its dipole perpendicular to the interface. Drawings of $\theta = 0$ orientations are shown for CHF_3 and CH_3F together with the additional one for CH_2F_2.

display only a very small minimum at the interface. The more polar systems show also a strong angular dependence of the solvation free energy, $\theta = 0$ being the preferred orientation

for CHF_3 and CH_3F whereas $\theta = 180°$ is preferred in case of CH_2F_2. For the two apolar molecules, a change in orientation does not affect the profile significantly as expected.

In Fig. 3 we have compared the $\theta = 0$ results with the MD simulations carried out by Pohorille and Wilson,[32] for the same interface. Pohorille and Wilson simulated the excess chemical potentials rather than solvation energies but the two quantities are in practice equivalent.[42] In order to facilitate the comparison, we have translated our profiles to match the solvation energy values obtained by the MD simulations in bulk hexane: absolute values are in this context of no importance as the profile across the interface is not affected.

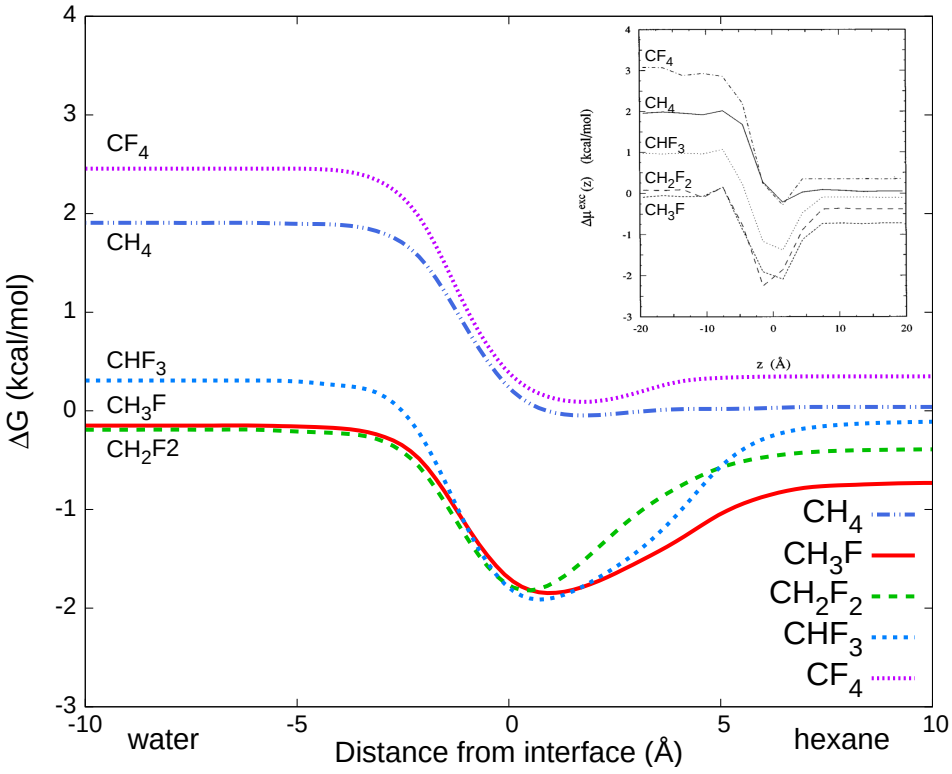

Figure 3: Comparison between the profiles of solvation free energy and excess chemical potentials for the $CH_xF_{(4-x)}$ set of molecules at the water-hexane. The insert reports the corresponding chemical potentials from ref.[32]. All values are in kcal/mol. For the sake of the comparison our results have been translated in the energy scale to match the solvation energy values in hexane reported by Garrett. The corrections (in kcal/mol) are as follows: -0.9765 for CH_4, -0.2734 for CH_3F, +0.6842 for CH_2F_2, +1.2724 for CHF_3, +0.9910 for CF_4

As can be seen from Fig. 3, the agreement between the two sets of calculations is generally good. For methane and CF_4 both methods predict that hexane is the preferred medium as

intuition would also dictate. In both calculations no significant minimum is seen at the interface for methane whereas a small minimum is present in both cases for CF_4. For the polar molecules both our calculations and MD simulations predict a surfactant behavior: the minima we have obtained are however less pronounced than those obtained by Pohorille and Wilson.

4.2 Solvation energy profiles of Set 2

The analysis of the second set of molecules at the vapor-water surface is first presented in terms of three separated groups of solutes (alcohols, gases, others) and finally compared with the simulations from Garrett *et al.*[33]

In Fig. 4 we report the calculated solvation free energy profiles at the water-vapor interface for the four investigated alcohols with two different orientations with respect to the interface. In order to elucidate the interplay of the different contributions to the solvation free energy, for ethanol we also report them separately.

For all alcohols, a surfactant behavior is found with free energy minima of the order of 1.5-3.5 kcal/mol with respect to the solvation free energy in bulk water. The orientation with the OH group pointing towards the water phase ($\theta = 0$) is clearly preferred for all alcohols (we note that for ethanediol due to its symmetry the two orientations are equivalent). Looking at the more detailed analysis reported for ethanol, we see that electrostatics shows no minimum at the interface: as expected most of the electrostatic energy is gained when the OH group crosses the interface. The aliphatic chain yields a modest but still negative contribution. Dispersion is also negative; however it unfolds gradually on a wider range. Repulsion, which is positive as expected, matches dispersion in extension but it is smaller in magnitude. Cavitation is obviously positive and its variation across the interface is sharper. The overall effect of the non-electrostatic contributions is therefore characterized by a minimum and a maximum. When electrostatics is also added, the minimum is accentuated whereas the maximum almost disappears. We conclude that the surfactant behavior

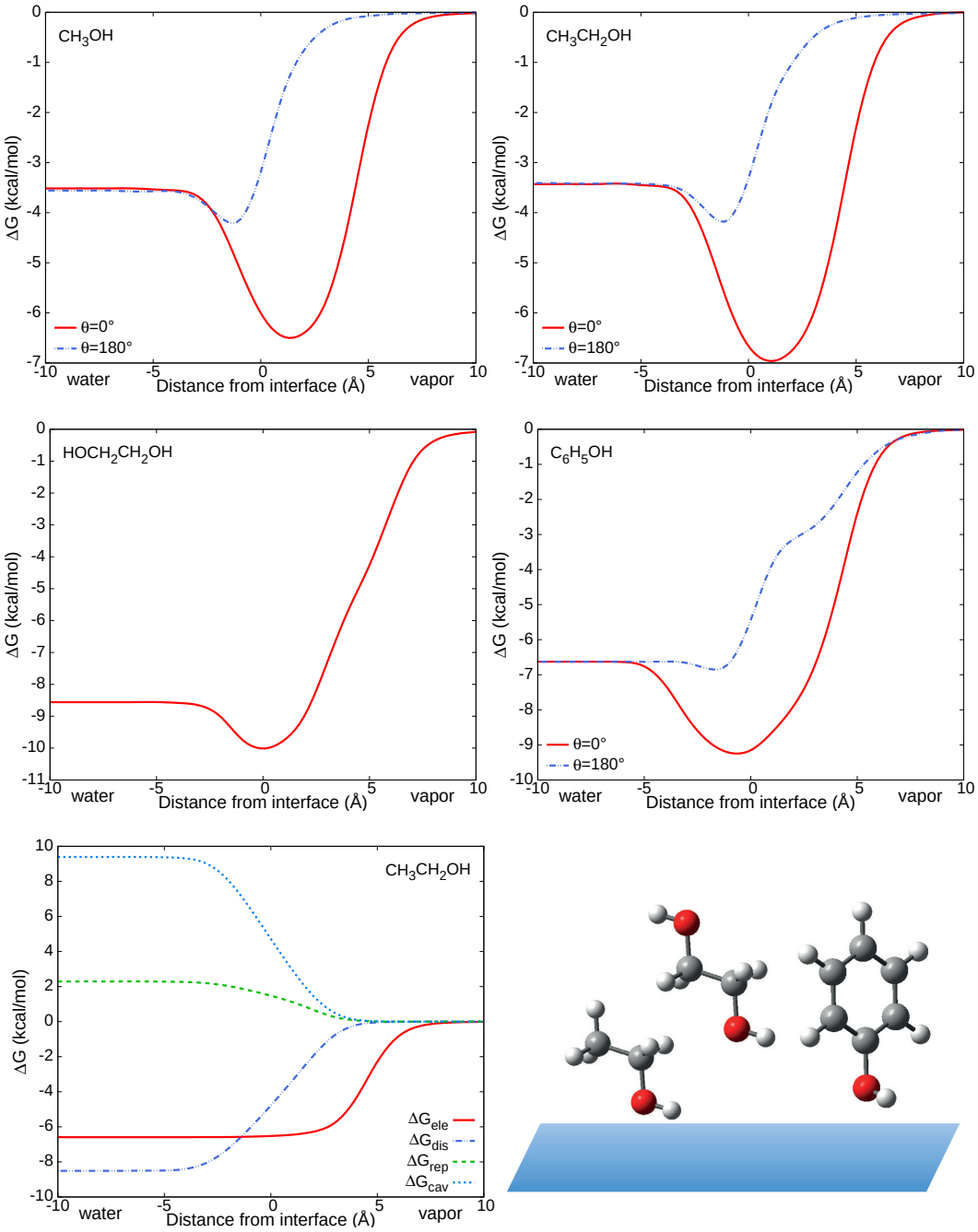

Figure 4: Solvation free energy profiles (in kcal/mol) for the four investigated alcohols at the water-vapor interface. The full and the dotted lines refer to $\theta = 0$ and $\theta = 180°$ orientation of the OH group, respectively. For ethanol we also report all the electrostatic and non-electrostatic contributions. Drawings of $\theta = 0$ orientations are also shown.

of ethanol and the other alcohols which show similar overall solvation profiles, is due to how the different contributions arise across the interface. In a previous work, Frediani et

al.[19] obtained similar results, albeit by making use of a semiclassical parameterization of non-electrostatic contribution and the original formulation of the PCM electrostatics.[22]

To better understand the effects of the orientation of the solute with respect to the interface we have selected ethanol and phenol and repeated the free energy profiles for different orientations. The results are reported in Fig. 5.

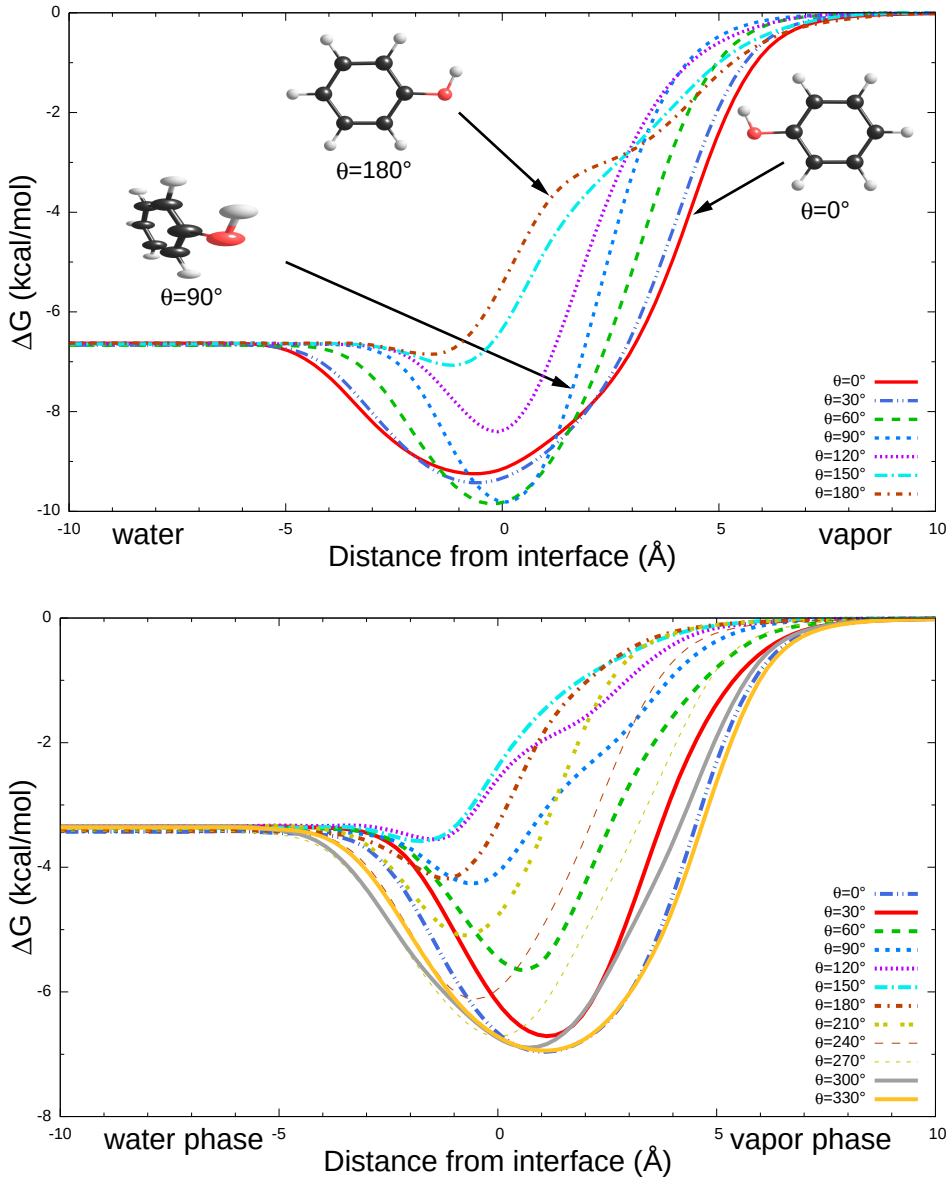

Figure 5: Free energy profiles (in kcal/mol) for the water-vapor transfer of phenol (a) and ethanol (b) at various θ angles. For phenol only half of the range of possible angles is shown, due to the symmetry of the system.

For phenol one can see that, when moving from air into bulk water, the most stable

orientation is initially $\theta = 0°$ (i.e. with OH group pointing towards the solution, see Fig. 2) while when the molecule is across the interface, the most stable orientation becomes $\theta = 90°$ – i.e. with the benzene ring lying flat on the surface. The most stable orientation changes again when phenol is deeper in the water phase ($\theta = 60°$). Further in bulk water, the $\theta = 0°$ orientation becomes preferred once again. Asymptotically, all orientations are obviously equivalent. This finding shows that throughout the transfer process the orientation changes gradually in order to maximize the solute solvent interaction: initially the electrostatic part, which is largest for the polar OH tail, dominates driving the phenol perpendicular to the interface ($\theta = 0°$). Close to the interface dispersion effects are maximized by allowing a larger portion of the molecule to be close to the solvent ($\theta = 90°$). Finally the molecule rotates again towards $\theta = 0°$ in order to delay the insurgence of the cavitation energy.

For ethanol, one can see that, when moving from air into the bulk water, the most stable orientation is $\theta = 330°$ (with OH group nearly pointing towards bulk). This orientation becomes energetically equivalent with $\theta = 0°$ shortly before the interface, where the OH group comes in contact with interfacial area. After passing the interface, the most stable orientation is $\theta = 270°$ (OH group pointing towards bulk). At extremes all orientations are, again, equivalent. In contrast to phenol, ethanol-interface orientation are preponderantly dominated by the electrostatic interaction between the polar hydroxilic group, therefore the variations in the orientation across the interface are in this case less pronounced.

Moving to the remaining compounds of Set 2, in Fig. 6 we report the profiles for the polar systems (DMSO, NH_3 and H_2O_2), whereas in Fig. 7 those for the apolar ones (O_2, N_2, O_3 and benzene).

For DMSO and ammonia (see Fig. 6) a similar behavior is found with respect to that observed for the alcohols. By contrast, hydrogen peroxide shows no surfactant behavior, and is strongly solvated in water, with relative ΔG of 12 kcal/mol. N_2, and benzene (see Fig. 7), do not show any preference for solvation, whereas O_2 and O_3 yield a solvation energy of -1 kcal/mol and -2.7 kcal/mol respectively. Among these molecule, only benzene shows

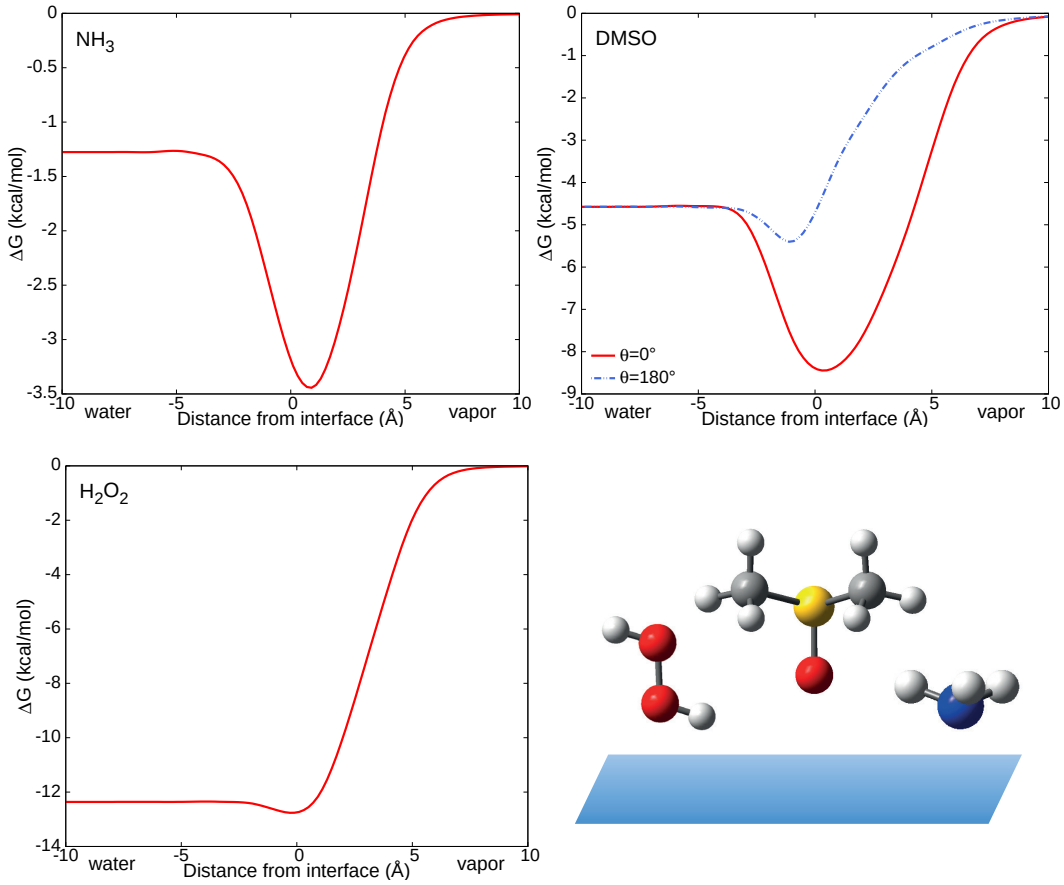

Figure 6: Solvation free energy profiles (in kcal/mol) for NH_3, DMSO and H_2O_2 at the water-vapor interface. The full and the dotted lines refer to $\theta = 0$ and $\theta = 180°$ orientations, respectively. Drawings of $\theta = 0$ orientations are also shown.

a significant surfactant behavior with an energy minimum at the surface of around -2.5 kcal/mol.

For the solutes of Set 2, a reference study was performed by Garrett et al.,[33] by means of Molecular Dynamics (MD). In their approach a 4-point profile for each molecule was generated, using free energy values in bulk water, at the barrier, at the interface and in vapor. As the reference MD data in this case is less detailed (only a few points for each solute), we have compared the small maximum we observed before going through interface, with the second MD point from the left (defined as the "barrier" by Garrett *et al.* [33]). Similarly we have compared the third point in the MD simulations with the minimum of our profile for each solute. The comparison between our profiles and those calculated by Garrett

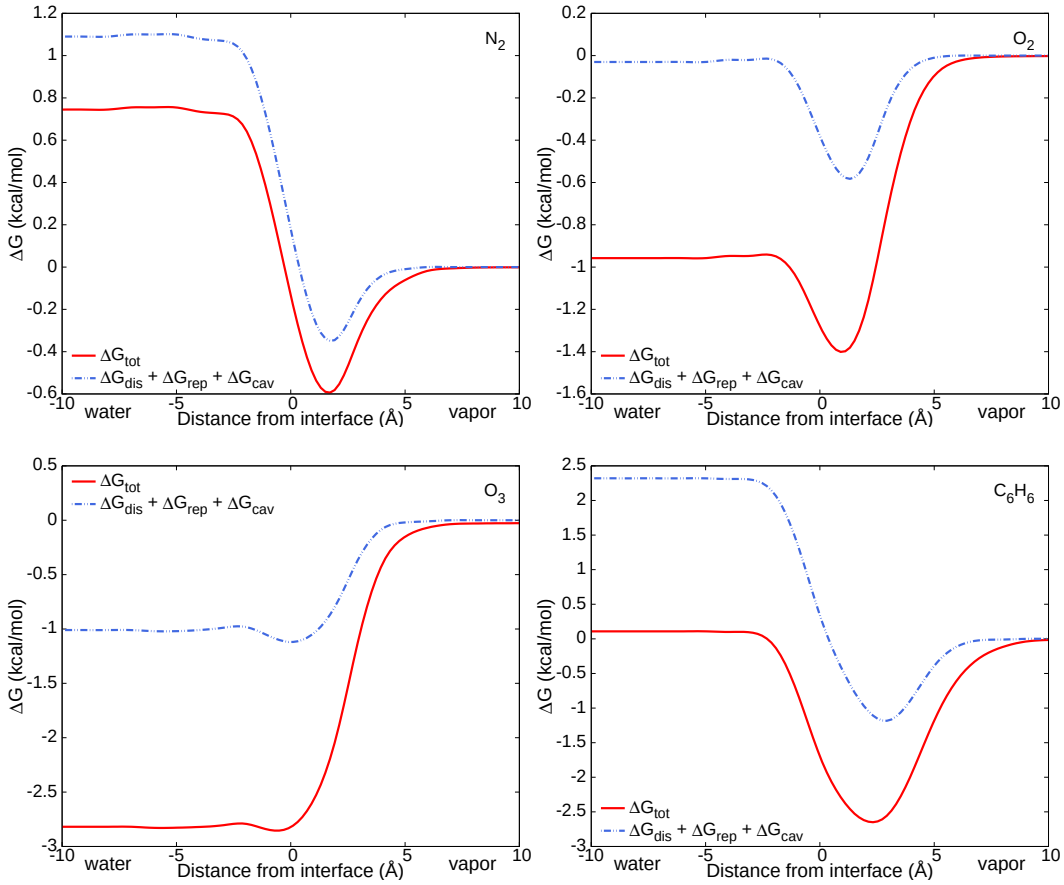

Figure 7: Solvation free energy profiles (in kcal/mol) for O_2, N_2, O_3 and benzene at the water-vapor interface. All curves refer to orientation with the molecular long axis perpendicular to the interface. Full lines refer to total solvation free energies whereas the dashed lines refer to the non-electrostatic contribution only.

et al. is shown in Fig. 8 for $\theta = 0$: for a more direct comparison we have rescaled the data reported in Fig. 4-Fig. 7 so to have free energies obtained in bulk of water as zero.

Our result show a good a semi-quantitative agreement with the MD simulations: the ordering of the various compounds in terms of solvation energy values is almost entirely reproduced, whereas the value of the minima do not entirely match the MD values. We stress that the comparison in the latter case is made more complicated by the lack of the full profile in the reference data. From a quantitative point of view, our free energy values are generally larger in absolute value with respect to those reported by Garrett et al.[33] A possible reason for the observed discrepancies is the lack of a proper description of hydrogen

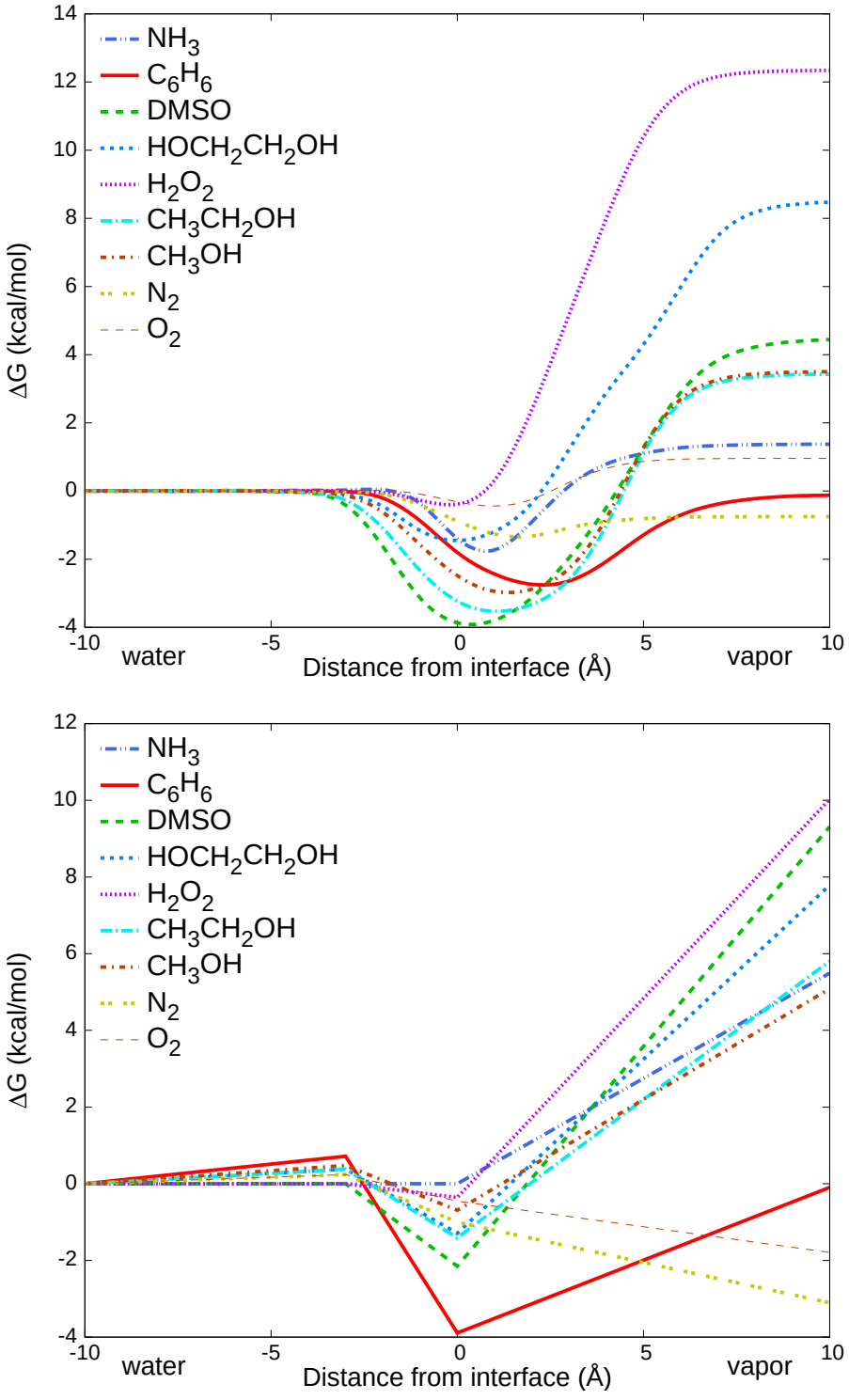

Figure 8: Free energy profiles (in kcal/mol) for water-vapor transfer of the molecules belonging to set 2. Graph (a): present work; graph (b): data extracted from Ref.[33]

bonding: each solute will be affected differently, depending on its ability to form hydrogen bonds with water.

5 Conclusions

We have presented an integrated QM/PCM approach to treat solvation at diffuse solvent surfaces and interfaces. All the main contributions to the solvation free energy (electrostatics, dispersion, repulsion) are included in a self consistent way into the QM description of the solute and made position-dependent as requested by the interfacial environment. For the remaining model-specific term, namely the energy required to create the molecular cavity hosting the solute, a completely classical correction to the energy is instead introduced. Also in this case, however, a position-dependent formulation is used. The approach has been tested by comparing solvation free energy profiles for the transfer of small molecules between two solvents and between vapor and water to those obtained with previous atomistic simulations available in the literature. The good agreement found in the two investigated sets of systems indicate both the feasibility and the semiquantitative accuracy of the approach, which can now be employed to investigate other systems. In this respect one relevant problem we intend to address is the interaction of molecules with the surface of water droplets, which is an essential component in the investigation of atmospheric chemistry processes.[43,44]

In addition, the inclusion of both the electrostatic and non-electrostatic interactions directly in the solute Hamiltonian makes the model a potential useful tool to study molecular properties and electronic processes at the interfaces, which is beyond the capabilities of simulation methods.

6 Acknowledgments

This work has been supported by the Research Council of Norway through a Centre of Excellence Grant (Grant No 179568/V30) and by the Tromsø Research Foundation (SURFINT

grant). Computer time from the Norwegian Super- compting Program (NOTUR) is also gratefully acknowledged.

Supporting Information

Parameterized β values for various solvents. This material is available free of charge via the Internet at http://pubs.acs.org.

References

(1) Tomasi, J.; Persico, M. Molecular Interactions in Solution: an Overview of Methods Based on Continuous Distributions of the Solvent. *Chem. Rev.* **1994**, *94*, 2027–2094.

(2) Tomasi, J.; Mennucci, B.; Cammi, R. Quantum Mechanical Continuum Solvation Models. *Chem. Rev.* **2005**, *105*, 2999–3093.

(3) Grimme, S. Density Functional Theory with London Dispersion Corrections. *WIREs: Comput. Mol. Sci.* **2011**, *1*, 211–228.

(4) Gordon, M. S.; Fedorov, D. G.; Pruitt, S. R.; Slipchenko, L. V. Fragmentation Methods: a Route to Accurate Calculations on Large Systems. *Chem. Rev.* **2012**, *112*, 632–672.

(5) Cramer, C.; Truhlar, D. Implicit Solvation Models: Equilibria, Structure, Spectra, and Dynamics. *Chem. Rev.* **1999**, *99*, 2161–2200.

(6) Floris, F.; Tomasi, J.; Ahuir, J. Dispersion and Repulsion Contributions to the Solvation Energy - Refinements to a Simple Computational Model in the Continuum Approximation. *J. Comput. Chem.* **1991**, *12*, 784–791.

(7) Tunon, I.; Ruiz-Lopez, M.; Rinaldi, D.; Bertran, J. Computation of Hydration Free Energies using a Parameterized Continuum Model: Study of Equilibrium Geometries and Reactive Processes in Water Solution. *J. Comput. Chem.* **1996**, *17*, 148–155.

(8) Curutchet, C.; Orozco, M.; Luque, F. Solvation in Octanol: Parametrization of the Continuum MST Model. *J. Comput. Chem.* **2001**, *22*, 1180–1193.

(9) Cramer, C. J.; Truhlar, D. G. A universal approach to solvation modeling. *Acc. Chem. Res.* **2008**, *41*, 760–768.

(10) Marenich, A. V.; Cramer, C. J.; Truhlar, D. G. Uniform Treatment of Solute–Solvent Dispersion in the Ground and Excited Electronic States of the Solute Based on a Solvation Model with State-Specific Polarizability. *J. Chem. Theory Comput.* **2013**, *9*, 3649–3659.

(11) Amovilli, C.; Mennucci, B. Self-Consistent-Field Calculation of Pauli Repulsion and Dispersion Contributions to the Solvation Free Energy in the Polarizable Continuum Model. *J. Phys. Chem. B* **1997**, *101*, 1051–1057.

(12) Weijo, V.; Mennucci, B.; Frediani, L. Toward a General Formulation of Dispersion Effects for Solvation Continuum Models. *J. Chem. Theory Comput.* **2010**, *6*, 3358–3364.

(13) Pomogaeva, A.; Chipman, D. M. New Implicit Solvation Models for Dispersion and Exchange Energies. *J. Phys. Chem. A* **2013**, *117*, 5812–5820.

(14) Andersson, Y.; Langreth, D.; Lundqvist, B. van der Waals Interactions in Density-Functional Theory. *Phys. Rev. Lett.* **1996**, *76*, 102–105.

(15) Cances, E.; Mennucci, B.; Tomasi, J. A New Integral Equation Formalism for the Polarizable Continuum Model: Theoretical Background and Applications to Isotropic and Anisotropic Dielectrics. *J. Chem. Phys.* **1997**, *107*, 3032–3041.

(16) Mennucci, B.; Cances, E.; Tomasi, J. Evaluation of Solvent Effects in Isotropic and Anisotropic Dielectrics and in Ionic Solutions with a Unified Integral Equation Method:

Theoretical Bases, Computational Implementation, and Numerical Applications. *J. Phys. Chem. B* **1997**, *101*, 10506–10517.

(17) Frediani, L.; Cammi, R.; Corni, S.; Tomasi, J. A polarizable continuum model for molecules at diffuse interfaces. *J. Chem. Phys.* **2004**, *120*, 3893.

(18) Frediani, L.; Mennucci, B.; Cammi, R. Quantum-Mechanical Continuum Solvation Study of the Polarizability of Halides at the Water/Air Interface. *J. Phys. Chem. B* **2004**, *108*, 13796–13806.

(19) Frediani, L.; Pomelli, C.; Tomasi, J. n-Alkyl Alcohols at the Water/Vapour and Water/Benzene Interfaces: a Study on Phase Transfer Energies. *Phys. Chem. Chem. Phys.* **2000**, *2*, 4876–4883.

(20) Rivail, J.-L.; Rinaldi, D. A Quantum Chemical Approach to Dielectric Solvent Effects in Molecular Liquids. *Chem. Phys.* **1976**, *18*, 233–242.

(21) Tapia, O.; Goscinski, O. Self-Consistent Reaction Field Theory of Solvent Effects. *Mol. Phys.* **1975**, *29*, 1653–1661.

(22) Miertuš, S.; Scrocco, E.; Tomasi, J. Electrostatic Interaction of a Solute with a Continuum. A Direct Utilizaion of ab initio Molecular Potentials for the Prevision of Solvent Effects. *Chemical Physics* **1981**, *55*, 117–129.

(23) Cances, E.; Mennucci, B. New Applications of Integral Equations Methods for Solvation Continuum Models: Ionic Solutions and Liquid Crystals. *Journal Of Mathematical Chemistry* **1998**, *23*, 309–326.

(24) Bondesson, L.; Frediani, L.; Agren, H.; Mennucci, B. Solvation of N-3(-) at the Water Surface: The Polarizable Continuum Model Approach. *J. Phys. Chem. B* **2006**, *110*, 11361–11368.

(25) Amovilli, C. Calculation of the Dispersion Energy Contribution to the Solvation Free-Energy. *Chem. Phys. Lett.* **1994**, *229*, 244–249.

(26) Curutchet, C.; Orozco, M.; Luque, F.; Mennucci, B.; Tomasi, J. Dispersion and Repulsion Contributions to the Solvation Free Energy: Comparison of Quantum Mechanical and Classical Approaches in the Polarizable Continuum Model. *J. Comput. Chem.* **2006**, *27*, 1769–1780.

(27) Pierotti, R. Scaled Particle Theory of Aqueous and Non-Aqueous Solutions. *Chem. Rev.* **1976**, *76*, 717–726.

(28) Stephens, P. J.; Devlin, F. J.; Chabalowski, C. F.; Frisch, M. J. Ab-Initio Calculation of Vibrational Absorption and Circular-Dichroism Spectra Using Density-Functional Force-Fields. *Journal Of Physical Chemistry* **1994**, *98*, 11623–11627.

(29) BECKE, A. D. Density-Functional Thermochemistry .3. the Role of Exact Exchange. *Journal of Chemical Physics* **1993**, *98*, 5648–5652.

(30) Frisch, M. J.; Trucks, G. W.; Schlegel, H. B.; Scuseria, G. E.; Robb, M. A.; Cheeseman, J. R.; Montgomery, J. A., Jr.; Vreven, T.; Kudin, K. N.; Burant, J. C. et al. Gaussian 03, Revision B.05. Gaussian, Inc., Wallingford, CT, 2004.

(31) Dunning, T. H. Gaussian-Basis Sets for Use in Correlated Molecular Calculations .1. the Atoms Boron Through Neon and Hydrogen. *Journal of Chemical Physics* **1989**, *90*, 1007–1023.

(32) Pohorille, A.; Wilson, M. Excess cCemical Potential of Small Solutes Across Water-Membrane and Water-Hexane Interfaces. *J. Chem. Phys.* **1996**, *104*, 3760–3773.

(33) Garrett, B.; Schenter, G.; Morita, A. Molecular Simulations of the Transport of Molecules Across the Liquid/Vapor Interface of Water. *Chem. Rev.* **2006**, *106*, 1355–1374.

(34) Paul, S.; Chandra, A. Binding of Hydrogen Bonding Solutes at Liquid-Vapour Interfaces of Molecular Fluids. *Chemical Physics Letters* **2004**, *400*, 515–519.

(35) Wilson, M.; Pohorille, A. Adsorption and Solvation of Ethanol at the Water Liquid-Vapor Interface: A Molecular Dynamics Study. *J. Phys. Chem. B* **1997**, *101*, 3130–3135.

(36) Taylor, R. S.; Ray, D.; Garrett, B. C. Understanding the Mechanism for the Mass Accommodation of Ethanol by a Water Droplet. *Journal of Physical Chemistry B* **1997**, *101*, 5473–5476.

(37) Taylor, R. S.; Garrett, B. C. Accommodation of Alcohols by the Liquid/Vapor Interface of Water: Molecular Dynamics Study. *Journal of Physical Chemistry B* **1999**, *103*, 844–851.

(38) Dang, L. X.; Feller, D. Molecular dynamics study of water-benzene interactions at the liquid/vapor interface of water. *Journal of Physical Chemistry B* **2000**, *104*, 4403–4407.

(39) Dang, L. X.; Garrett, B. C. Molecular mechanism of water and ammonia uptake by the liquid/vapor interface of water. *Chemical Physics Letters* **2004**, *385*, 309–313.

(40) Vacha, R.; Slavicek, P.; Mucha, M.; Finlayson-Pitts, B. J.; Jungwirth, P. Adsorption of Atmospherically Relevant Gases at the Air/Water Interface: Free Wnergy Profiles of Aqueous Solvation of N-2, O-2, O-3, OH, H2O, HO2, and H2O2. *Journal of Physical Chemistry A* **2004**, *108*, 11573–11579.

(41) Vieceli, J.; Roeselova, M.; Potter, N.; Dang, L. X.; Garrett, B. C.; Tobias, D. J. Molecular Dynamics Simulations of Atmospheric Oxidants at the Air-Water Interface: Solvation and Accommodation of OH and O3. *The Journal of Physical Chemistry B* **2005**, *109*, 15876–15892.

(42) Ben-Naim, A.; Mazo, R. Size dependence of solvation Gibbs energies: A critique and a rebuttal of some recent publications. *J. Phys. Chem. B* **1997**, *101*, 11221–11225.

(43) Martins-Costa, M. T. C.; Anglada, J. M.; Francisco, J. S.; Ruiz-Lopez, M. F. Reactivity of Atmospherically Relevant Small Radicals at the Air-Water Interface. *Angew. Chem. Int. Ed.* **2012**, *51*, 5413–5417.

(44) Martins-Costa, M. T. C.; Anglada, J. M.; Francisco, J. S.; Ruiz-Lopez, M. F. Reactivity of Volatile Organic Compounds at the Surface of a Water Droplet. *J. Am. Chem. Soc.* **2012**, *134*, 11821–11827.